

Chiral phase transition in lattice QCD as a metal-insulator transition

Antonio M. García-García

*Physics Department, Princeton University, Princeton, New Jersey 08544, USA and
The Abdus Salam International Centre for Theoretical Physics, P.O.B. 586, 34100 Trieste, Italy*

James C. Osborn

Physics Department & Center for Computational Science, Boston University, Boston, MA 02215, USA

We investigate the lattice QCD Dirac operator with staggered fermions at temperatures around the chiral phase transition. We present evidence of a metal-insulator transition in the low lying modes of the Dirac operator around the same temperature as the chiral phase transition. This strongly suggests the phenomenon of Anderson localization (localization by destructive quantum interference) drives the QCD vacuum to the chirally symmetric phase in a way similar to a metal-insulator transition in a disordered conductor. We also discuss how Anderson localization affects the usual phenomenological treatment of phase transitions *a la* Ginzburg-Landau.

PACS numbers: 72.15.Rn, 71.30.+h, 05.45.Df, 05.40.-a

One of the most important features of the infrared limit of the strong interactions is the spontaneous breaking of the approximate chiral symmetry. The order parameter associated with this spontaneous chiral symmetry breaking (S χ SB) is the chiral condensate, $\langle\bar{\psi}\psi\rangle$, which in the absence of S χ SB would vanish as the quark mass goes to zero. In nature the lightest quarks are not massless so a nonzero condensate is expected even in a free theory. However the small quark mass can only account for a small percentage of the chiral condensate, the rest has its origin in the strong non-perturbative color interactions of QCD. Although lattice simulations have already provided overwhelming evidence that S χ SB is a feature of QCD it is still highly desirable to understand its origin in more simple terms.

Simplified models of QCD where gauge configurations are given by instantons have played a leading role in the description of the S χ SB [1, 2, 3]. Instantons [4], originally introduced in QCD by t'Hooft [5] to solve the so called $U(1)$ problem, are classical solutions of the Euclidean Yang-Mills equations of motion. Their relation with the S χ SB stems from the fact that the QCD Dirac operator has an exact zero eigenvalue in the field of an instanton. In the QCD vacuum, these zero modes coming from different instantons mix together to form a band around zero. It turns out the spectral density, $\rho(\lambda)$, of the Dirac operator in this region is directly related to the chiral condensate through the Banks-Casher relation [6],

$$\begin{aligned}\langle\bar{\psi}\psi\rangle &= -\lim_{m\rightarrow 0}\lim_{V\rightarrow\infty}\int_0^\infty\frac{2m}{m^2+\lambda^2}\frac{\rho(\lambda)}{V}d\lambda \\ &= -\lim_{\lambda\rightarrow 0}\lim_{V\rightarrow\infty}\frac{\pi\rho(\lambda)}{V},\end{aligned}\quad (1)$$

where V is the space-time volume. Based on this result it was shown that the instanton contribution was capable of producing a nonzero chiral condensate with a value close to the phenomenological one [2, 3] (see [7] for a detailed review).

For sufficiently high energies the non-abelian gauge in-

teraction of QCD is weak (asymptotic freedom) and chiral symmetry is restored. This poses an interesting question: How is the chiral symmetry restored as we go from low to high energies or, equivalently, from low to high temperatures? A standard approach to the chiral phase transition is to invoke universality arguments [8], namely, it is assumed that the transition is controlled by symmetries rather than by the dynamical details of QCD. The chiral phase transition is then studied by looking at the most general renormalizable Ginzburg-Landau Lagrangian with the chiral symmetries of QCD. By using a perturbative renormalization group analysis, Pisarsky and Wilczek [8] found that for two massless flavors the transition is expected to be second order. However, for three or more flavors, it was conjectured to be first order due to the absence of infrared stable fixed points in the renormalization group equations. The order and the very existence of the chiral transition is also sensitive to details such as the mass of the light quarks and whether the above mentioned $U(1)$ symmetry is restored at the same temperature as the chiral one.

Generally speaking it is still under debate to what extent effective models only based on universality arguments provide an accurate description of the chiral phase transition [9] (see e.g. [10] for a recent discussion of some lattice results). For instance, it is unclear how interactions, still important at the transition [11], modify this picture or whether the ϵ expansion used to compute the critical exponents can be extrapolated to the limit, $\epsilon = 1$, relevant for QCD.

In this paper we present evidence that the phenomenon of Anderson localization [12] (localization by destructive quantum interference) plays a crucial role in the chiral restoration. We suggest that localization drives the system to the chirally symmetric phase in a way similar to a metal-insulator transition (also referred to as Anderson transition (AT)) in a disordered conductor. Anderson localization thus counterbalances the effect of the QCD interactions which tend to keep the S χ SB phase. For the sake of completeness we briefly review some basic facts

about disordered systems (see section VI of [13] for a review) in the context of condensed matter before relating them to QCD.

Localization properties of a disordered system can be investigated by looking at the eigenstates or, more economically, by studying level statistics of the Hamiltonian. In two and lower dimensions, destructive interference caused by backscattering produces exponential localization of the eigenstates in real space for any amount of disorder. As a consequence, quantum transport is suppressed, the spectrum is uncorrelated (Poisson statistics) and the system becomes an insulator. In more than two dimensions there exists a metal-insulator transition for a critical amount of disorder. By critical disorder we mean a disorder such that, if increased, all the eigenstates become exponentially localized. For a disorder strength below the critical one, the system has a mobility edge at a certain energy which separates localized from delocalized states. Its position moves away from the band center as the disorder is decreased. Delocalized eigenstates, typical of a metal, are extended through the sample and their level statistics agree with the random matrix theory (RMT) prediction for the appropriate symmetry. We note that in the case of QCD the role of Hamiltonian is played by the Dirac operator.

Localization has already been investigated in lattice QCD. The low lying modes of lattice QCD with overlap fermions at zero temperature were found to be localized even though the eigenvalue spectrum agrees with the random matrix prediction [14]. This gives an apparent contradiction since the RMT also predicts extended eigenstates. Conversely, simulations with staggered fermions do find extended states along with an eigenvalue spectrum that agrees with RMT [15], though the localization properties of the low modes have not previously been studied in detail near the chiral phase transition. In the context of instanton liquid models (ILM) at zero temperature, the $S\chi$ SB has been related to the conductivity (delocalization) in a disordered medium [16, 17, 18, 19]. At nonzero temperature, we have recently reported [20] that the chiral phase transition in the ILM is induced by an AT of the lowest lying eigenmodes of the Dirac operator. In this letter we show that the close relations between Anderson localization and the chiral phase transition found in the ILM holds in full lattice QCD as well.

In the next section we introduce the lattice simulations used in this paper and present evidence of a localization transition in quenched lattice QCD. Then we show that this metal-insulator transition occurs around the same temperature as the chiral restoration. In section III we repeat the analysis in full (unquenched) lattice QCD with similar results. The last section provides some further clarifications about the relation between Anderson localization and chiral restoration including the effect of *à la* Ginzburg-Landau.

I. LOCALIZATION OF THE QCD DIRAC OPERATOR AT NONZERO TEMPERATURE

In this section we investigate how the localization properties of the QCD Dirac operator depend on temperature. Specifically we are looking for a critical temperature at which a metal-insulator transition occurs. We shall also investigate if the spectral and eigenfunction properties around the critical region are compatible with those of a disordered conductor at the metal-insulator transition.

Our first task is to obtain both the eigenvalues and eigenvectors of the Dirac operator for different temperatures and then find the location, if any, of the metal-insulator transition. In principle one should also determine the spectral region in which the transition takes place. In the quenched case, according to the Banks-Casher relation, the physics of the $S\chi$ SB and its eventual restoration is exclusively linked with the lowest eigenmodes of the Dirac operator so we will look for the metal-insulator transition only in this region. For dynamical fermions the situation is different, the condensate depends on a wider spectral region, so we will examine how much the region in which the AT occurs overlaps with the one relevant for the chiral condensate.

A. Details of the lattice QCD simulations

For the present study we have used quenched and 2+1 flavor lattices at couplings (β) around the chiral restoration transition. Both sets of lattices were generated using a one-loop Symanzik improved gauge action [21]. The lattice sizes used are $L^3 \times 4$ where L is the spatial size and the number of time slices is always 4. The quenched lattices used $L = 16$ and 20 while the unquenched lattices used $L = 12$ and 16. The 2+1 flavor lattices were generated using the a^2 tadpole improved “asqtad” staggered Dirac operator [22] with 2 light quark flavors and 1 strange quark flavor with the light quark masses one tenth the strange quark mass. The $L = 12$ lattices come from the MILC collaboration and are a subset of the ones mentioned in [23]. The $L = 16$ lattices were generated using the same parameters as the smaller lattices except for the volume.

We have obtained the lowest 64 eigenvalues and eigenvectors of the asqtad staggered Dirac operator on these lattices. In the quenched lattices we first rotated the gauge fields by an appropriate Z_3 transformation so that the Polyakov loop is in the “real” phase. This avoids having to deal with seeing separate transitions for the different phases at different temperatures, although it would be interesting to examine the other phases too. We note that the staggered Dirac operator actually represents four copies of the continuum Dirac operator (called “tastes”) that are mixed together. However, since the lattice spacing is large, the scale for the taste breaking is much larger than the eigenvalues being studied here. It is thus expected that the eigenvalues behave as if from

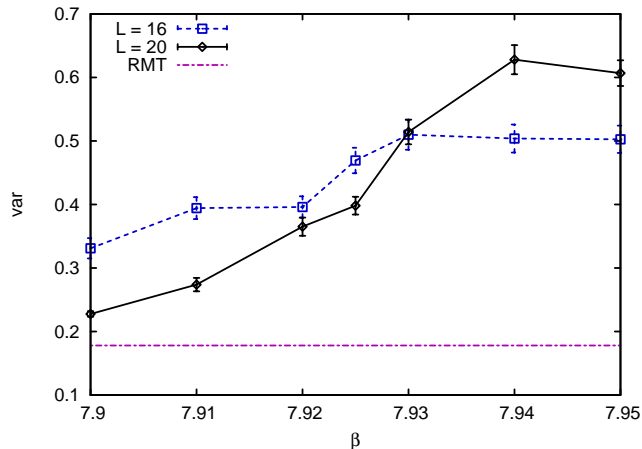


FIG. 1: Level spacing variance (var) of the low eigenvalues of the Dirac operator in quenched QCD for two volumes ($L^3 \times 4$) and values of the lattice coupling β spanning the transition. The system undergoes a metal-insulator transition around $\beta_c \sim 7.93$.

a single continuum Dirac operator confined to the topological sector $\nu = 0$.

B. Eigenvalue analysis in quenched QCD

The critical temperature at which the AT close to the origin occurs was determined by performing a finite size scaling analysis [24]. In essence this method consists of computing a spectral correlator for different sizes and then seeing for what value of the temperature it becomes scale invariant (no dependence on the size). We recall that scale invariance is a typical signature of the AT. Since we are interested in a small spectral window close to the origin we have chosen a short range correlator, the level spacing distribution $P(s)$ [25]. This is the probability of finding two neighboring eigenvalues at a distance $s_i = (\lambda_{i+1} - \lambda_i)/\Delta$, with Δ being the local mean level spacing. For an insulator, levels are not correlated, there is no level repulsion and $P(s) = e^{-s}$. In the case of a metal there is level repulsion, $P(s) \sim s^\alpha$ ($s \ll 1$), and Gaussian decay $P(s) \sim e^{-4s^2/\pi}$ ($s \gg 1$) with α an integer depending on the symmetry of the Dirac operator ($\alpha = 2$ in our case).

In order to avoid any dependence on bin size in the spacing distribution, the scaling behavior of $P(s)$ is examined through its variance,

$$\text{var} \equiv \langle s^2 \rangle - \langle s \rangle^2 = \int_0^\infty ds s^2 P(s) - 1, \quad (2)$$

where $\langle \dots \rangle$ denotes spectral and ensemble averaging. The prediction for a metal (from RMT) is $\text{var}_M \approx 0.178$ while an insulator (Poisson statistics) gives $\text{var}_I = 1$. If the variance gets closer to the metal (insulator) result as the volume is increased we say that the system is delo-

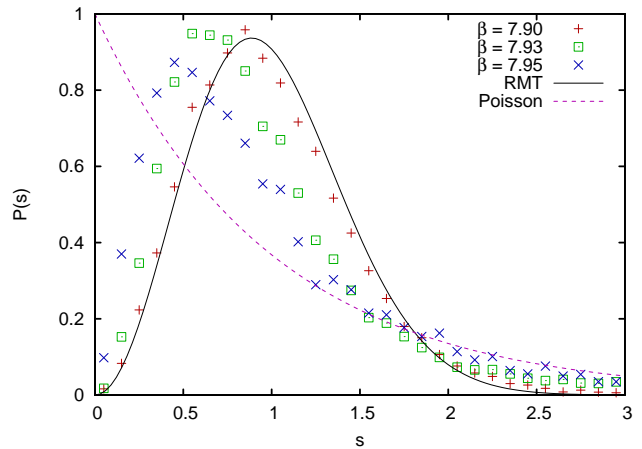


FIG. 2: Level spacing distribution, $P(s)$, of the low eigenvalues of the Dirac operator in quenched QCD for lattice size $20^4 \times 4$ and values of the coupling around the transition. A transition from the random matrix prediction (RMT) typical of a metal towards the Poisson result typical of an insulator is observed as the temperature is increased (increasing β).

calized (localized). Any other intermediate value of var in the thermodynamic limit is a signature of a metal-insulator transition.

In figure 1 we plot the variance of the eigenvalues in the interval $a\lambda \in [0.025, 0.05]$ (with a the lattice spacing) for different volumes and couplings. Increasing β corresponds to increasing temperature. The variance appears to be scale invariant at $\beta = 7.93$ and increases (decreases) with the volume for larger (smaller) β . This behavior points to a metal-insulator transition around $\beta_c \sim 7.93$ for this interval. The interval above was chosen so as to contain enough eigenvalues to obtain good statistics for all couplings used. Other intervals give similar results provided that we remain sufficiently close to the origin although the value of β_c may decrease slightly as the interval approaches zero. Note also that as β increases the lattice spacing a decreases which, in turn, increases the eigenvalue range in physical units. We have not tried to correct it in the quenched case as it would not affect the scaling with volume seen at fixed β which is how the localization properties and β_c are determined. However we mention this is likely the cause of the downward bend in figure 1 for $\beta = 7.95$.

Evidence of a metal-insulator transition is also seen directly in the level spacing distribution shown in figure 2. This is plotted for the largest volume lattices ($20^3 \times 4$) at different β along with the metal (RMT) and insulator (Poisson) results. As the temperature is increased the distribution moves from metallic towards an insulator similarly to the variance. Note that, as with the variance plot, the system has still not reached the result of an insulator at this volume, but should scale towards it as the volume is increased.

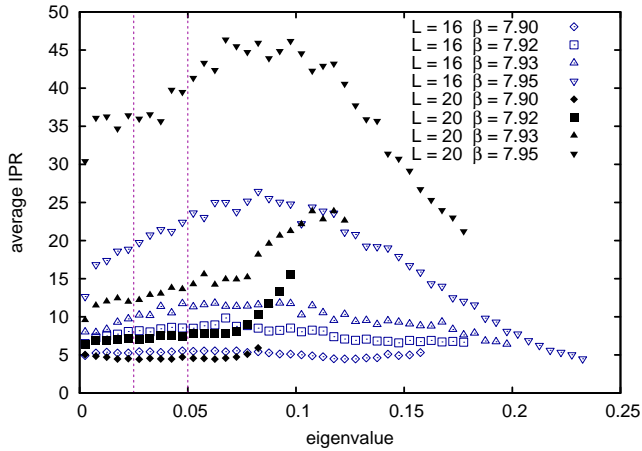


FIG. 3: The average inverse participation ratio (IPR) versus the eigenvalue (in lattice units) for the low eigenvalues of the Dirac operator in quenched QCD for two volumes ($L^3 \times 4$) and values of the lattice coupling β spanning the transition. The scaling of IPR with the volume suggests that an AT takes place around $\beta_c \sim 7.92 - 7.93$ (see text). The dotted lines show the eigenvalue range considered for locating the localization transition in the quenched lattices.

C. Eigenvector analysis in quenched QCD

We now investigate whether eigenstate properties are compatible with the findings of the previous section. We recall that extended eigenstates are a signature of a metal and exponential localization is typical of an insulator. The eigenstate decay is very sensitive to statistical fluctuations, boundary conditions and finite size effects in general and consequently it is not the best alternative for numerical investigations. A much simpler option is to study the scaling with volume of the eigenstate moments, $P_q = L^{d(q-1)} \int d^{d+1}r |\psi_\lambda(r)|^{2q}$, where $\psi_\lambda(r)$ is a normalized eigenstate of the Dirac operator with eigenvalue λ and d is the spatial dimension. In a metallic sample it is expected that P_q decreases with volume approaching $P_q \sim 1$ in the thermodynamics limit. Conversely in an insulator, P_q is expected to increase with volume as $P_q \propto L^{d(q-1)}$. At the AT, eigenstates are multifractal meaning the wavefunction moments present anomalous scaling with respect to the sample size, $P_q \propto L^{-(D_q-d)(q-1)}$, where D_q is a set of exponents describing the transition [26, 27]. For the analysis of the lattice data we restrict ourselves to the second moment, P_2 , usually referred to as the inverse participation ratio (IPR). In figure 3 we plot the average of the IPR versus eigenvalue for different volumes and couplings. We observe that for $\beta \leq 7.92$ (≥ 7.93) the IPR decreases (increases) with the volume. This suggests, in agreement with the previous spectral analysis, that an AT takes place around $\beta_c \sim 7.93$. Unfortunately the range of accessible volumes is too small to provide a reliable estimate of the multifractal dimensions, D_q , in the critical region.

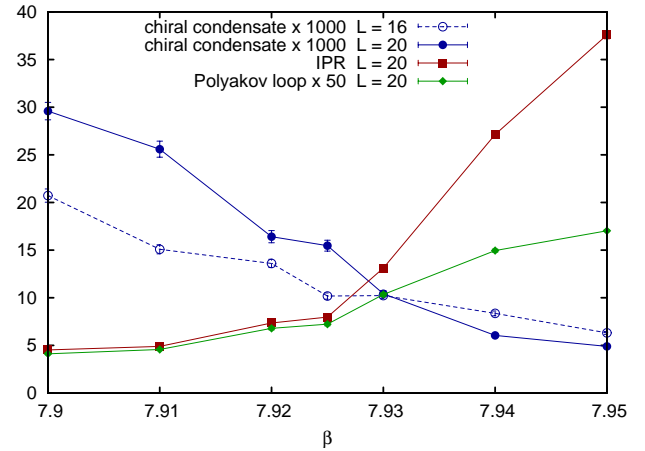


FIG. 4: Chiral condensate, IPR of the low eigenmodes and Polyakov loop in quenched QCD for lattice sizes $L^3 \times 4$ and values of the lattice coupling β spanning the transition. Remarkably the localization, chiral restoration and deconfinement transitions all occur around the same temperature.

II. LOCALIZATION AND CHIRAL RESTORATION IN QUENCHED LATTICE QCD

Having found that an AT close to the origin does occur in quenched QCD we now investigate its possible relation with the chiral phase transition. Although in the quenched case there is no true chiral symmetry, it is still possible to study the quenched chiral condensate. From the Banks-Casher relation (1) we know that the condensate in the chiral limit is proportional to the density of eigenvalues of the Dirac operator near zero. By chiral restoration it is thus meant that the infrared limit of the spectral density of the Dirac operator vanishes at a certain temperature. Using this definition of the condensate we can then approximate the density of eigenvalues near zero simply from the average of the smallest eigenvalue. The precise relation can be obtained from the RMT prediction of the distribution of the smallest eigenvalue [28]. We will then compare the behavior of the quenched chiral condensate to the localization transition in QCD.

In figure 4 we plot the quenched chiral condensate, the average IPR of the low modes, and the real part of the average Polyakov loop at different couplings. Amazingly the indicators for chiral symmetry restoration, Anderson localization and deconfinement (respectively) all show signs of a transition around the same temperature. We have shown the condensate for two different volumes so the scaling to infinite volume can be seen. As the volume increases the condensate increases for $\beta < 7.93$ and decreases for $\beta > 7.93$ suggesting that the chiral transition occurs around $\beta_c \sim 7.93$. This behavior is very similar to that found in the level spacing variance shown in figure 1.

The IPR in figure 4 is averaged over modes in the same eigenvalue range used in the previous section. In agree-

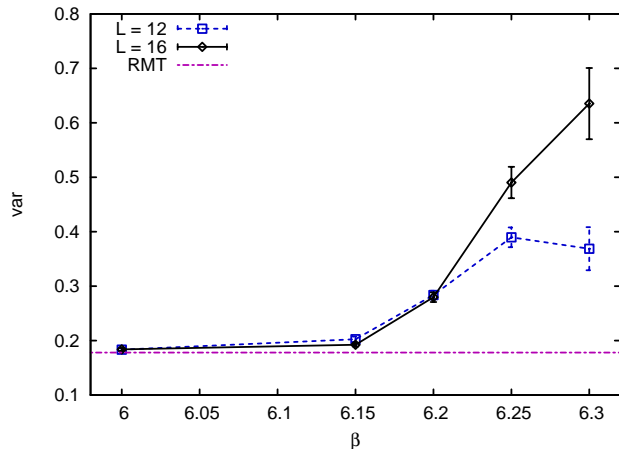


FIG. 5: Level spacing variance (var) of the low eigenvalues of the Dirac operator in 2+1 flavor QCD for two volumes ($L^3 \times 4$) and values of the lattice coupling β spanning the transition. The system undergoes a metal-insulator transition around $\beta_c \sim 6.2$.

ment with figure 3 we again see that it rises abruptly around the same β_c . Although we can't currently provide any direct connection between the localization transition and deconfinement, it is still interesting to see that the order parameter for confinement (the Polyakov loop) shows an extremely similar behavior to the IPR thus suggesting that the two transitions are also related. Additionally, as is shown above, we do see evidence that there is a connection between localization and the chiral phase transition. Indeed, the apparent agreement in critical temperatures strongly suggests that Anderson localization is the mechanism driving the chiral phase transition in quenched QCD.

III. LOCALIZATION AND CHIRAL RESTORATION IN FULL LATTICE QCD

We now examine the localization transition in full lattice QCD. With respect to the chiral transition the most important difference from the quenched case is the fact that, for nonzero quark masses, the condensate is no longer exclusively determined by the eigenmodes close to the origin. The condensate now gets contributions from larger eigenvalues with a relative weight given in (1). The importance of the modes right at zero then becomes diluted by the nonzero modes. Only in the chiral limit, as the dynamical mass approaches zero, does the condensate only depend on the lowest modes. Therefore in order to understand the relationship between localization and chiral restoration we must study the localization properties over a range of eigenmodes similar to the ones relevant for the condensate. Typically this spectral window comprises not only critical eigenstates at the mobility edge but also localized and delocalized eigenstates around it. The issue of whether such a mixture causes a crossover

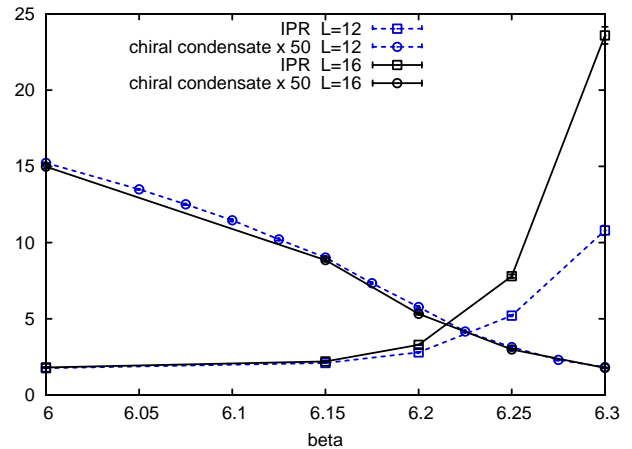


FIG. 6: Chiral condensate for the light (u, d) quarks and IPR of the low eigenmodes for 2 + 1 flavor QCD for two volumes ($L^3 \times 4$) and values of the lattice coupling β spanning the transition. The IPR shows signs of an AT around $\beta_c \sim 6.2$ while the condensate shows only a crossover.

or a transition is subtle and requires further study.

Understanding the relationship between localization and $S\chi SB$ in full QCD is also complicated by the fact that at the physical quark masses the chiral transition is really a rapid crossover. The critical temperature in this case is usually defined by the maximum of the chiral susceptibility. However, as discussed below, the localization properties are related to the susceptibility and thus could still provide a connection between the two phenomena.

In order to explore this scenario our first task is to locate the mobility edge in full lattice QCD. For this we look at the level spacing variance (2) for two different lattice sizes versus coupling (figure 5) in a range of eigenvalues $0 \leq \lambda \leq 30$ MeV (the relation for the lattice spacing in [23] was used to convert to physical units). This range goes up to roughly three times the light quark mass and thus covers an important fraction of the contribution to the condensate. Our results are not sensitive to the length of the spectral interval utilized provided that there is no coexistence of localized and delocalized eigenstates. If this occurs we shall observe a crossover rather than a transition.

Here we clearly see that the variance is close to the random matrix prediction typical of a metal for $\beta < 6.2$ while for $\beta > 6.2$ it tends rapidly to the result of Poisson statistics typical of an insulator. Thus around $\beta_c \sim 6.2$ there is a transition from the metallic to the insulator limit. Converting this to physical units we get $T_c \sim 195$ MeV. By transition we really mean that there is a sharp increase of the variance in a quite narrow window of temperatures. Much larger volume would be needed to clarify whether it is just a crossover or a true transition.

We see a similar scaling behavior in the IPR (figure 6). Again there is a transition from extended to localized states at around the same $\beta_c \sim 6.2$. However if we look at the chiral condensate also plotted on the same

figure we see that it does not show any volume dependence. This is in agreement with the expected behavior at a chiral crossover. In this case one can still define the critical temperature from the maximum of the chiral susceptibility. For the unquenched lattices this is about 194 MeV [29], which compares favorably with that found for the AT.

The reason why a transition is observed for localization can be understood fairly easily. For the localization transition, a mobility edge forms at zero for some temperature and then moves towards higher energies as the temperature is increased. If the mobility edge is below the spectral window being studied then the states will appear extended and if above then they will appear localized. While the mobility edge is inside the window there will be a mix of extended, critical and localized eigenmodes. This will technically give a crossover, however this is merely a consequence of the size of the spectral window analyzed which is related to the dynamical quark mass. From the point of view of localization theory the determination of what constitutes a large and small window is governed by the rate of change of the mobility edge with temperature which, for our case, seems to be very fast. Thus if the window around the mobility edge is small enough a true transition is expected.

However the reason why we observe a crossover in the chiral transition is less clear. The spectral region which the chiral condensate is sensitive to is also determined by the quark mass. Evidently due to the nonzero mass, the chiral transition is not as sensitive to the mobility edge itself but rather to the coexistence of localized, delocalized and critical eigenmodes in the spectral region of interest. Since we find that both phenomena occur at the same temperature, it is natural to expect that Anderson localization is still responsible for causing the chiral transition. However the exact nature of the relationship is still under investigation.

In summary, our numerical results show that an AT occurs in the low energy part of the Dirac eigenmodes at around the same temperature as the chiral transition. This is fully consistent with the idea of Anderson localization as the microscopic mechanism driving the chiral phase transition. However much larger lattices and better statistics are still needed to fully explore this scenario, and especially to extract the spectrum of multifractal dimensions and critical exponents.

IV. ADDITIONAL DISCUSSION ON LOCALIZATION AND CHIRAL RESTORATION

This final section is devoted to a more detailed account on how localization and the chiral phase transition are related. We start by addressing certain problems associated to linking these two phenomena. The most serious one is the fact that the spectral density is not a good order parameter for the transition to localization since it does not vanish in any of the phases. Signatures of

the transition to localization are typically found in correlation functions of higher order. By contrast the chiral condensate is directly related to the spectral density of the Dirac operator through the Banks-Casher relation (1). This seems to suggest that Anderson localization and the chiral phase transition cannot be so intimately related. However, in disordered systems with chiral symmetry (or any other additional discrete symmetry) the spectral density is already sensitive to the strength of disorder [30, 31] so it may still play the role of an order parameter for the transition. Additionally the fluctuations of the order parameter are related to density-density correlations which are sensitive to localization effects even in systems with no chiral symmetry.

Another issue that deserves further clarification is the choice of the term Anderson localization. In the context of disordered systems, this term is used if localization is produced by destructive interference. On the other hand the term Mott transition refers to a transition caused by interactions. Quark interactions are a key ingredient in QCD so it may seem more appropriate to use Mott-Anderson instead of Anderson. We stick to Anderson to emphasize that disorder, due to the fluctuations of gauge fields, plays a crucial role in the transition as well. An indication that this is the case is the fact that even for temperatures just above chiral restoration, QCD is still non-perturbative [11] thus suggesting the mechanism driving the transition is not exclusively a weakening of the strong interactions.

Finally we discuss whether the order and critical exponents of the phase transition can be deduced from the study of localization. In the case of the standard non-chiral AT evidence that some sort of phase transition takes place is the fact that the localization length diverges at the transition with a certain universal critical exponent ν . Also the spectrum of multifractal dimensions D_q at the AT must be related to certain critical exponents of the chiral phase transition. For instance, the susceptibility is given by the integral of a density-density correlation function whose decay is controlled by the multifractal dimension D_2 [32].

We recall that critical exponents related to D_q cannot be predicted by any mean field theory even if perturbative corrections are taken into account. Unfortunately the range of volumes used here is still too small to provide a reliable estimate of the multifractal dimensions D_q in the critical region and its relation to critical exponents. However in the context of ILM [20] it has already shown that, at the chiral phase transition, eigenvectors of the QCD Dirac operator are multifractal with a D_q similar to the one found in a 3D disordered conductor at the AT. This is another indication that the standard picture of the chiral transition as a simple second (or first) order phase transition may be a oversimplification. The idea we want to put forward is that not only symmetry but also Anderson localization are necessary ingredients to understand the chiral phase transition.

In conclusion, we have studied Anderson localization of

the QCD Dirac operator at nonzero temperature. Near the origin we found a clear transition from delocalized to localized states as the temperature is increased. Around this mobility edge, the eigenvectors and spectral correlations are similar to those of a disordered system undergoing an AT. Remarkably both the transition to localization and the chiral phase transition occur at the same temperature. This indicates that the phenomenon of Anderson

localization plays a crucial role in the restoration of the chiral symmetry.

AMG thanks C. Gatttringer, M. Teper and B. Bringoltz for illuminating discussions. JCO thanks C. DeTar and L. Levkova for data and discussions pertaining to the MILC lattices. AMG was supported by a Marie Curie Outgoing Fellowship, contract MOIF-CT-2005-007300. JCO was supported in part by U.S. DOE grant DE-FC02-01ER41180.

-
- [1] C.G. Callan, R. Dashen and D.J. Gross, Phys. Rev. D **17**, 2717 (1978).
 - [2] D. Diakonov and V. Petrov, Nucl. Phys. **B245**, 259 (1984).
 - [3] E. Shuryak, Nucl. Phys. **B203**, 93,116,140 (1982).
 - [4] A. Belavin, A. Polyakov, A. Schwartz and Y. Tyupkin, Phys. Lett. **59**, 85 (1975).
 - [5] G. 't Hooft, Phys. Rev. Lett. **37**, 8 (1976).
 - [6] T. Banks and A. Casher, Nucl. Phys. **B169**, 103 (1980).
 - [7] T. Schäfer and E. Shuryak, Rev. Mod. Phys. **70**, 323 (1998).
 - [8] R.D. Pisarski and F. Wilczek, Phys. Rev. D **29**, 338 (1984).
 - [9] H. Meyer-Ortmanns, Rev. Mod. Phys. **68**, 473 (1996).
 - [10] T. Mendes, hep-lat/0609035.
 - [11] E.V. Shuryak and I. Zahed, Phys. Rev. C **70**, 021901 (2004).
 - [12] P.W. Anderson, Phys. Rev. **109**, 1492 (1958).
 - [13] T. Guhr, A. Mueller-Groeling and H.A. Weidenmueller, Phys. Rept. **299**, 189 (1998).
 - [14] R.G. Edwards, U.M. Heller, J. Kiskis and R. Narayanan, Phys. Rev. Lett. **82**, 4188 (1999); E.-M. Ilgenfritz, K. Koller, Y. Koma, G. Schierholz, T. Streuer and V. Weinberg, Nucl. Phys. (Proc. Suppl.) **153**, 328 (2006).
 - [15] P.H. Damgaard, U.M. Heller and A. Krasnitz, Phys. Lett. B **445**, 366 (1999); C. Bernard, *et. al.*, PoS **LAT2005**, 299 (2005).
 - [16] D. Diakonov and P. Petrov, Phys. Lett. B **147**, 351 (1984); Sov. Phys. JETP **62**, 431 (1985); Nucl. Phys. **B272**, 457 (1986).
 - [17] J.C. Osborn and J.J.M. Verbaarschot, Phys. Rev. Lett. **81**, 268 (1998); Nucl. Phys. **B525**, 738 (1998).
 - [18] R.A. Janik, M.A. Nowak, G. Papp and I. Zahed, Phys. Rev. Lett. **81**, 264 (1998).
 - [19] A.M. Garcia-Garcia and J.C. Osborn, Phys. Rev. Lett. **93**, 132002 (2004).
 - [20] A.M. Garcia-Garcia and J.C. Osborn, Nucl. Phys. **A770**, 141 (2006).
 - [21] K. Symanzik, *Recent developments in gauge theories*, eds. G. 't Hooft, *et. al.*, Plenum, New York, 313 (1980).
 - [22] K. Orginos and D. Toussaint, Phys. Rev. **D59**, 014501 (1999); Nucl. Phys. (Proc. Suppl.) **73**, 909 (1999); G. P. Lepage, Nucl. Phys. (Proc. Suppl.) **60A**, 267 (1998); Phys. Rev. D **59**, 074502 (1999).
 - [23] C. Bernard, *et. al.*, PoS **LAT2005**, 156 (2005).
 - [24] B.I. Shklovskii, *et. al.*, Phys. Rev. B **47**, 11487 (1993).
 - [25] M.L. Mehta, *Random Matrices*, Academic Press, New York, 2nd edition (1991).
 - [26] F. Wegner, Z. Phys. B **36**, 209 (1980); B.L. Altshuler, V.E. Kravtsov and I.V. Lerner, *Mesoscopic Phenomena in Solids*, eds. B.L. Altshuler, *et. al.*, North Holland, Amsterdam (1991); V.I. Falko and K.B. Efetov, Europhys. Lett. **32**, 627 (1995).
 - [27] A.D. Mirlin, *et. al.*, Phys. Rev. E **54**, 3221 (1996); F. Evers and A.D. Mirlin, Phys. Rev. Lett. **84**, 3690 (2000); E. Cuevas, *et.al.*, Phys. Rev. Lett. **88**, 016401 (2002).
 - [28] S. M. Nishigaki, P. H. Damgaard and T. Wettig, Phys. Rev. D **58**, 087704 (1998).
 - [29] L. Levkova (MILC Collaboration), private communication.
 - [30] A.M. García-García and K. Takahashi, Nucl. Phys. **B700**, 361 (2004); A. Parshin and H.R. Schober, Phys. Rev. B **57**, 10232 (1998).
 - [31] A.M. Garcia-Garcia and J.J.M. Verbaarschot, Nucl. Phys. **B586**, 668 (2000).
 - [32] V.E. Kravtsov and K.A. Muttalib, Phys. Rev. Lett. **79**, 1913 (1997); S. Nishigaki, Phys. Rev. E **59**, 2853 (1999).